

Electrochemical Treatment of Phenolic Wastewater with TiO₂/SnO₂ Electrode: Influence of Operating Parameters and Optimization

Hui Yuan^{1,2,*}, Haiming Li², Liwei Zhao², Jiyue Chen²

¹ Tianjin Eco-Environmental Monitoring Center, No. 19 Fukang Road, Nankai District, Tianjin, 300191, China

² Jiuzhou Environment Technology (Tianjin) Co.,Ltd. No. 20 Huaming Avenue, Dongli District, Tianjin, 300300, China

*E-mail: yuanhui15022089006@163.com

Received: 5 November 2019 / Accepted: 17 December 2019 / Published: 10 February 2020

The phenolic wastewater produced in the production process generally has the characteristics of high concentration, strong biological toxicity, difficult degradation and long residual period, making it one of the priority pollutants with prominent environmental risks to be monitored. Electrochemical treatment of phenolic wastewater is characterized by high current efficiency, simple equipment, mild reaction conditions and clean process. In this paper, the working electrode was prepared with ordinary graphite plate as the electrode lining and TiO₂ supported by SnO₂ as the working outer layer, forming the relevant electrochemical reactor. Taking the simulated wastewater containing phenol as the research object, the technical condition, effect and related mechanism of electrochemical treatment of phenol wastewater were discussed.

Keywords: Electrochemical treatment; Phenol; Wastewater; Optimization; TiO₂/SnO₂ electrode

1. INTRODUCTION

With the rapid development of economy, the amount of industrial wastewater is increasing. The components of these industrial wastewater are complex, and most of them contain carcinogenic, teratogenic and mutagenic highly toxic pollutants, which will cause serious harm to the natural environment and human life and health [1–4]. Effective treatment and recycling of this kind of wastewater can not only relieve the pressure of water shortage in China, but also reduce the threats of various pollutants to the natural environment and human survival. The discharge of industrial organic wastewater mainly comes from petrochemical industry, coking industry, food industry, pharmaceutical

industry, printing and dyeing industry, textile industry, leather industry, papermaking industry and agriculture industry [5,6]. According to its pollutant composition, industrial organic wastewater can be divided into two categories: easy biodegradable wastewater and difficult biodegradable wastewater. Wastewater that is difficult to biodegrade generally contains toxic substances that retard or inhibit the growth of microorganisms. Pollutant indicators are usually described by biological oxygen consumption (BOD) and chemical oxygen consumption (COD) [7–10].

Biodegradable organic pollutants mainly refer to organic matters that cannot be decomposed at a very slow rate or at all during biochemical treatment, or even inhibit the growth of microorganisms. They mainly include polycyclic aromatic hydrocarbons, heterocyclic compounds, organochlorides, organophosphorus and various organic dyes [11–14]. The main reason why biodegradable organic wastewater is difficult to be biochemically treated is determined by its own characteristics. Due to the complex chemical composition and structure of these organisms, the lack of specific enzymes in the microbial community makes them resistant to degradation. In addition, organic pollution in this kind of waste water is toxic or can inhibit the growth of microorganisms, which cannot effectively survive and grow in this kind of waste water.

The commonly used methods for the treatment of biodegradable organic wastewater include physicochemical, biochemical and advanced oxidation techniques [15–18]. With the further research on this kind of wastewater treatment technology, advanced electrochemical oxidation technology has been developed because of its high efficiency, especially electrocatalytic oxidation technology has been paid more and more attention by researchers. Conventional electrochemical techniques include electrocatalytic oxidation, electroreduction and electroflocculation [19,20]. The treatment of refractory organic wastewater is mainly through electrocatalytic oxidation.

Electrocatalytic oxidation is the direct oxidation of organic pollutants on the surface of electrode materials with electrocatalytic properties during electrolysis. Alternatively, electrode materials can produce free radical groups with strong oxidation ability to indirectly oxidize organic pollutants in wastewater through electrochemical action, and finally make it completely degraded into harmless CO₂ and H₂O. Electrocatalysis means that the decorations on the electrode surface or in the solution phase can promote or inhibit the redox reaction of gaining and losing electrons on the working electrode under the action of electric field, while the decorations on the electrode surface or in the solution phase do not happen by themselves [21–25]. The electrocatalytic process mainly produces hydroxyl radical ($\cdot\text{OH}$), superoxide radical ($\cdot\text{O}_2$) and other active groups oxidize and degrade organic pollutants in wastewater. As an environmentally friendly technology, electrochemical oxidation has many advantages compared with other water treatment processes. Free radicals generated in electrochemical processes react directly with organic pollutants in wastewater [26–31]. The electron transfer of oxidation reaction is only completed between the electrode material and organic pollutants, and no oxidation agents need to be added. In the end, there are no toxic and harmful intermediate products in the reaction system, effectively avoiding the problem of secondary pollution. The electrochemical process is generally carried out under normal temperature and pressure, and the reaction conditions are mild. The electrochemical reaction conditions can be adjusted only by changing the applied current and voltage. In the process of electrochemical treatment of wastewater, the cooperative treatment of anode and cathode can be realized.

In the electrochemical process, gas flotation, flocculation, sterilization, disinfection and other functions are often held [32–36].

As the core of electrochemical process, electrode material is the main factor affecting electrochemical wastewater treatment. The performance of electrode not only affects the efficiency and cost of electrochemical process, but also directly determines whether the electrochemical oxidation degradation process is carried out. The degradation of organic pollutants must be realized through anode reaction. The catalytic performance of anode materials directly determines the efficiency of electrocatalytic oxidation. In this study, TiO₂-graphite plate working electrode was formed with ordinary graphite plate as electrode lining and TiO₂ as working outer layer. Then, SnO₂ was formed on the TiO₂-graphite plate working electrode surface for treating phenol wastewater. The results showed excellent catalytic activity and treatment effect as well as the practical application value in industrial wastewater treatment.

2. EXPERIMENTAL

For TiO₂-graphite plate working electrode was prepared using sol-gel adsorption method. At room temperature, 10 mL Ti(OC₄H₉)₄ were added to the mixture of 30 mL anhydrous ethanol and 2 mL acetic acid, and the mixture was continuously stirred for 30 min to obtain the uniform and transparent pale yellow solution (A). Slowly add 0.5 mL of HNO₃ into the mixture solution of 1 mL water and 10 mL anhydrous ethanol to obtain the solution (B) of p H≈3. Under intense agitation, solution (B) was added to solution (A) slowly at the speed of about 1 ~ 2 drops/sec. After 1 h, uniform and transparent pale yellow TiO₂ sol was obtained and aged for 6 h. TiO₂ sol slowly drops onto the graphite plate at a certain speed. After full adsorption, it is dried in an oven at 80°C. Finally, TiO₂-graphite plate electrode can be obtained by calcining at 500°C for 2 h in the atmosphere of nitrogen.

A small amount of HCl was used to dissolve an appropriate amount of SnCl₄·5H₂O, and anhydrous ethanol was added to prepare the coating solution. Soak TiO₂-graphite plate electrode in the coating solution, keep them for 1 min, then take them out and put them in a 120°C oven to dry for 10 min. Then put the working plate into a high-temperature hot oxidation furnace with set temperature for 15 min. After cooling to room temperature, soak, dry and heat oxidize again for 15 times. After the last soaking and drying, annealing to room temperature in muffle furnace at a constant temperature for 1 h to obtain the TiO₂-SnO₂-graphite plate electrode. The molar concentration of Ti in this region was between 0.2 ~ 0.8 mol/L, that is, stable and uniform TiO₂ sol was prepared. Therefore, TiO₂ sol was prepared with Ti molar concentrations of 0.3, 0.5 and 0.7 mol/L, and TiO₂-SnO₂-graphite was prepared by sol-gel-adsorption method, which was recorded as TiO₂-SnO₂-graphite-3, TiO₂-SnO₂-graphite-5 and TiO₂-SnO₂-graphite-7, respectively.

For wastewater degradation, The volume of wastewater degradation electrolytic cell was 100 mL. The anode was TiO₂-SnO₂-graphite plate electrode. The cathode is graphite plate. The effective area of both electrodes is 10 cm² and the polar distance is 2 cm. During the experiment, 50 mL phenol solution and 30 mL sodium sulfate solution were added to the electrolytic cell, and the two electrodes were kept parallel and immersed vertically in the electrolyte. The two electrodes were stirred magnetically, the DC

power was turned on, the current and voltage were adjusted to the required conditions, and the timing began. In this paper, continuous degradation method was adopted, and 1 mL samples were taken for determination every 15 min. The whole experiment was conducted at 25°C.

COD was determined by potassium dichromate method. The determination of H₂O₂ was carried out by titanium spectrophotometry. Phenol and aromatic intermediate products were determined by HPLC. Working conditions: Accurasil C18 column (4.6 mm×150 mm, 5 microns, UV detector). The mobile phase was methanol and 0.5 mM H₂SO₄ aqueous solutions, with a volume ratio of 4:6. The detection wavelength was 270 nm. Analysis method: 1 mL samples were taken from the electrolytic cell every 15 min, 0.1 mL methanol was added as an inhibitor, and then diluted with deionized water to a constant volume of 10 mL. Water samples were filtered with a 0.45 μm filter membrane, and then water samples were directly injected with a volume of 20 μL. The concentration of the standard sample and its peak area in HPLC were plotted as the standard curve. According to the concentration of phenol in the sample before and after electrolysis, the degradation rate was calculated (see the following formula), where C₀ and C_t were respectively the concentration of phenol (mg/L) before and after electrolysis t.

$$\text{Degradation rate} = \frac{C_0 - C_t}{C_0} \times 100\%$$

3. RESULTS AND DISCUSSION

Figure 1A shows the linear voltammetry curve of three electrodes of graphite plate, TiO₂-graphite plate and TiO₂-SnO₂-graphite plate in blank solution of 0.0075 mol/L Na₂SO₄. As can be seen from the figure, the current density of Na₂SO₄ aqueous solution on the graphite plate electrode was the smallest at the same electrode potential, and the current density of Na₂SO₄ aqueous solution on the TiO₂-SnO₂-graphite plate electrode was higher than that of TiO₂-graphite plate. The order of oxygen evolution potential of the three electrodes was TiO₂-SnO₂-graphite plate > TiO₂-graphite plate > graphite plate.

Figure 1B shows the linear voltammetry curves of the three electrodes in 100 mg/L phenol solution (with 0.0075 mol/L sodium sulfate as the supporting electrolyte). As shown in the figure, at the same potential, the phenol solution current density on TiO₂-SnO₂-graphite plate electrode was the highest, followed by TiO₂-graphite plate electrode, and the graphite plate electrode was the lowest. Therefore, TiO₂-SnO₂-graphite plate electrode is the best electrode material for phenol electrooxidation system.

When TiO₂ thin film is prepared by sol-gel, swelling and cracking are very easy to occur, and even flake off from the support [37–39]. The original ratio of sol is closely related to the cracking of gel. According to the complete phase diagram of Ti(OC₄H₉)₄-C₂H₅OH-H₂O system, the preparation of the film should be in the impregnated zone of the phase diagram [40,41]. These electrodes were then used as anodic oxidation of phenol in electrochemical reaction system. As can be seen from Figure 2A, when TiO₂-SnO₂-graphite-3, TiO₂-SnO₂-graphite-5 and TiO₂-SnO₂-graphite-7 were used as anodes, their degradation rates of phenol were different.

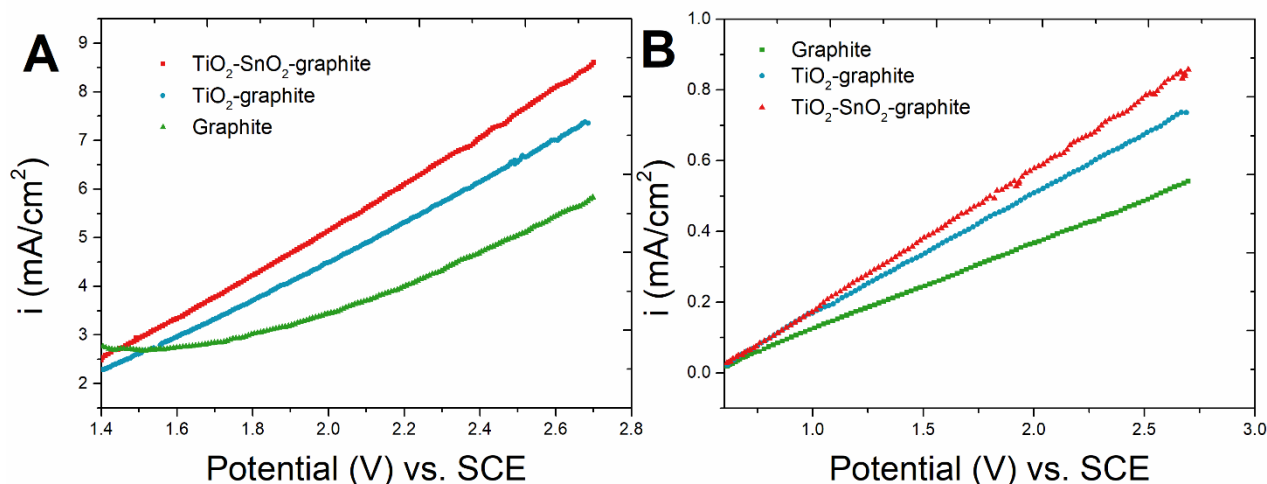


Figure 1. (A) Linear voltammograms of graphite plate, TiO₂-graphite plate and TiO₂-SnO₂-graphite plate in Na₂SO₄ solution. (B) Linear voltammograms of graphite plate, TiO₂-graphite plate and TiO₂-SnO₂-graphite in phenol solution.

When the concentration of titanium increased from 0.3 mol/L to 0.5 mol/L, the degradation rates of phenol also increased, but continued to increase to 0.7 mol/L, the degradation rates decreased. The amount of hydroxyl radicals produced by the three electrodes in Figure 2B is consistent with their trend of degradation rate of phenol. It is because of the different amount of hydroxyl radicals produced on the anode that the degradation rate of phenol is different. This may be because TiO₂-SnO₂-graphite-5 has a higher original supporting rate (the higher the concentration of titanium sol is, the higher the supporting rate is) and the best supporting fastness. Therefore, TiO₂-SnO₂-graphite-5 plate was selected as the anode of electrochemical oxidation of phenol.

Figure 2C shows the effect of TiO₂-SnO₂-graphite-5 on the degradation rate of phenol when it was used as the anode, cathode and anode, respectively. It can be seen that TiO₂-SnO₂-graphite-5 had the highest degradation rate when it was used as the anode. TiO₂-SnO₂-graphite-5 (1.3 cm x 5.7 cm) is divided into two equal area, bonding at the anode and cathode respectively, electrolytic 15 min, the phenol degradation rate negative (10.8%), indicating that some of phenol from TiO₂-SnO₂-graphite-5. When TiO₂-SnO₂-graphite-5 was used as the cathode, the degradation rate of phenol was lower (-56.8% at 15 min) in the same electrolysis time, that is, more phenol was desorption from the electrode into the solution. In general, the oxidation of phenol leads to the production of benzoquinone and organic acids which can be tested by HPLC. The organic acids would be completely mineralized into CO₂ and H₂O if they are further oxidized [42–44]. The degree of mineralization could be calculated by the carbon molar mass balance before and after electrochemical oxidization reaction [45–47]. Therefore, TiO₂-SnO₂-graphite-5 was adhered to the anode graphite plate in this system as the anode of electrochemical oxidation of phenol.

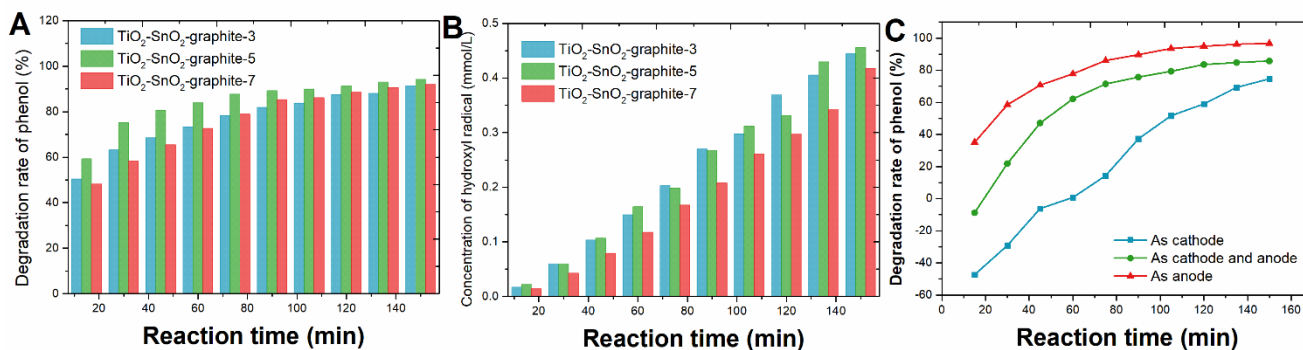


Figure 2. Effects of three different anodes on (A) phenol degradation rate and (B) hydroxyl free production. (C) Effect of TiO₂-SnO₂-graphite-5 as anode, cathode and anode on degradation rate of phenol.

For textile dyeing wastewater treatment, pH served the opposite effects on the color and COD removal by anodic oxidation and indirect oxidation. For anodic oxidation, the removal efficiency decreased with increasing pH possibly due to the enhancement of the side reaction of oxygen evolution. For indirect oxidation, the removal efficiency increased with increasing pH, attributing to the electrochemical production of H₂O₂ in a more alkaline solution [48,49]. The solution pH also changes the surface charge properties of nano TiO₂. Therefore, pH plays an important role in TiO₂-SnO₂-graphite plate electrode electrochemical oxidation of phenol. The electrooxidation effect of phenol at pH: 2, 6 and 10 was compared. Results as shown in Figure 3, degradation rate of phenol gradually accelerated with the decrease of initial solution pH. After 60 min reaction, the degradation rate of phenol was about 87.9% when pH was 2. The removal rate of phenol was 81.7% when pH was 6. When pH was 10, the degradation rate decreased sharply to 55.4%. It can be seen that the electrochemical degradation rate of phenol in acidic or neutral solution is higher than that in alkaline solution. The reason may be that H₂O₂ and ·OH are produced in the medium acidic solution. These highly oxidizing active substances accelerate the oxidation of phenol on the electrode. In alkaline solutions, diffused oxygen has difficulty gaining electrons to reduce the concentration of H₂O₂ produced. At the same time, the ·OH produced by the catalyst anode will be removed by hydroxide and carbonate in the alkaline solution.

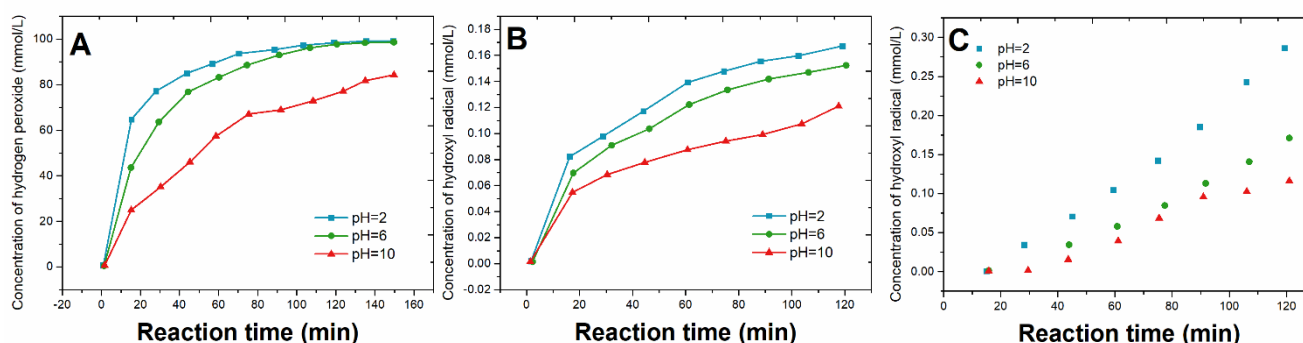


Figure 3. Effects of initial pH on (A) degradation of phenol, (B) concentration of H₂O₂ and (C) ·OH.

The degradation effect of phenol with Na_2SO_4 as electrolyte was studied when the concentration of Na_2SO_4 was 0.0375, 0.0750 and 0.1125 mol/L, respectively. As shown in Figure 4A, when the concentration of Na_2SO_4 increased from 0.0375 to 0.0750 mol/L, the degradation rate of phenol increased from 64.1% to 84.2% after 60 min of electrolysis. The degradation rate reached the highest when the concentration was 0.0750 mol/L. This is because the increase in electrolyte concentration increases the mass transfer coefficient and reduces energy consumption. However, when the concentration continued to increase to 0.1125 mol/L, the degradation rate decreased to 66.4%. Possibly due to the increase in electrolyte content, a large amount of SO_4^{2-} adsorbed on the electrode surface, which hindered the electrode reaction catalyzed by TiO_2 to produce $\cdot\text{OH}$. Meanwhile, the reaction between SO_4^{2-} and $\cdot\text{OH}$ reduced the concentration of $\cdot\text{OH}$, thereby reducing the oxidation of phenol on the electrode. The hydroxyl radicals generated were apt to electrophilically attack the adjacent or para position of phenol to produce hydroquinone and catechol, which as the main intermediates were easily further oxidized to p-benzoquinone [50,51]. Under further oxidation by the hydroxyl radicals, the conjugate structure of the benzene ring from p-benzoquinone would be disconnected and produced maleic acid, oxalic acid and other small molecules acid.

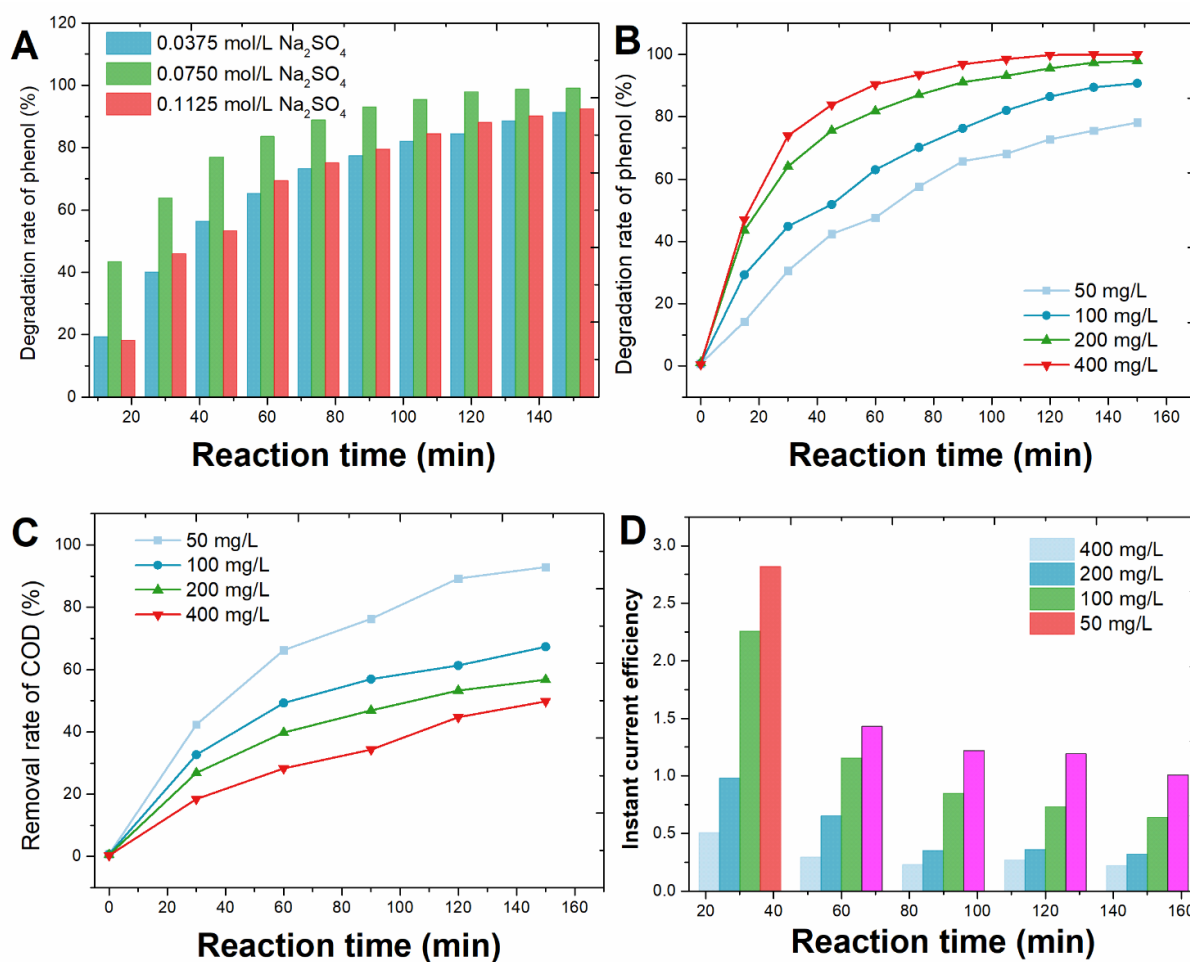


Figure 4. (A) Effect of Na_2SO_4 concentration on phenol degradation. Effects of initial phenol concentration on rates of (B) phenol degradation and (C) COD removal. (D) Effect of initial phenol concentration on instant current efficiency.

Figure 4B-C shows the change of phenol and COD in the electrocatalytic system with time when the initial concentrations of phenol were 50 mg/L, 100 mg/L, 200 mg/L and 400 mg/L, respectively. According to Figure 4B, with the increase of phenol concentration, the reaction rate constant decreased and the degradation rate decreased. The degradation rates were 87.2%, 84.3%, 60.6% and 47.2% respectively. COD removal rate also showed the same change rule (Figure 4B), and the corresponding COD removal rate was 65.2%, 52.1%, 42.4% and 31.5% respectively. Similar phenomenon was observed on the removal of wastewater, where the COD removal was incomplete when the dye concentration exceeded a certain value and required a higher current or a longer treatment time [52]. This indicates that more intermediate products are produced when the concentration is higher, and it is more beneficial for the complete mineralization of phenol when the concentration is lower.

Figure 4D shows the relationship between current efficiency and initial concentration of phenol. As can be seen from the figure, the current efficiency increased with the increase of initial concentration of phenol. This is because phenol not only has a direct oxidation reaction on the surface of TiO₂-SnO₂-graphite plate anode, but also has an indirect oxidation reduction reaction between phenol in solution and ·OH produced by anode. Moreover, the higher the initial concentration of phenol, the greater the degree of indirect reaction and the higher the current efficiency.

As can be seen from Figure 5, the degradation rates of phenol by the three electrodes were 83.1%, 67.5% and 44.2% at the time of electrolysis for 60min. Due to the conductivity and catalytic property of TiO₂, it was adhered to the graphite plate, and compared with the graphite plate electrode without TiO₂, the catalytic degradation of phenol on the electrode was accelerated. On the one hand, TiO₂-SnO₂-graphite plate electrode provided a three-dimensional space, increased the contact area between phenol and electrode, and enriched phenol molecules in TiO₂-SnO₂ substrate, which accelerated the migration of phenol molecules fixed in the substrate to the surface of adjacent TiO₂ catalyst. On the other hand, due to the high oxygen evolution potential of semiconductor TiO₂, the energy loss caused by the generation of oxygen was reduced, thus increasing the production of ·OH.

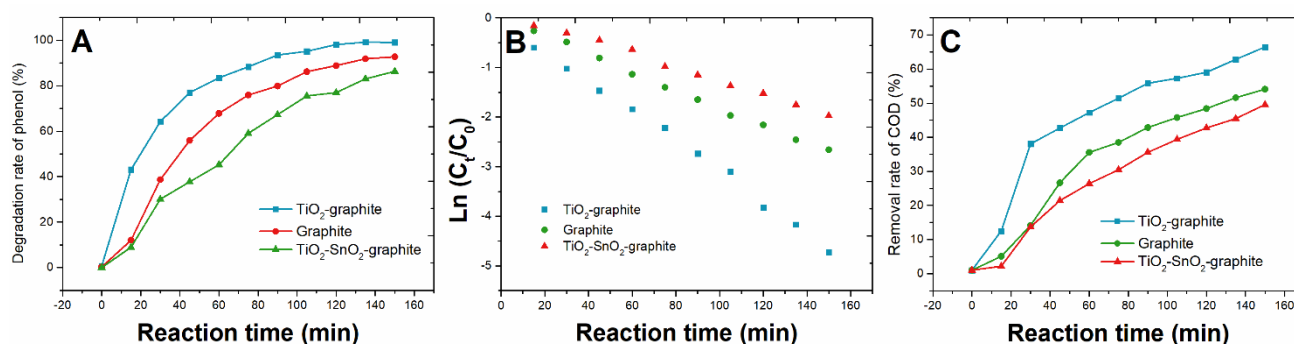


Figure 5. The effects of graphite plate, TiO₂-graphite plate and TiO₂-SnO₂-graphite plate as anodes on (A) degradation rate of the phenol, (B) kinetics and (C) removal rate of COD.

In order to analyze the mechanism of oxidation of phenol by three working electrodes, detect the presence of ·OH in electrochemical reaction process, and compare the ability of each electrode to

generate $\cdot\text{OH}$. In this experiment, p-hydroxybenzoic acid (4-hba) was used as the capture agent of $\cdot\text{OH}$, and the production rate of $\cdot\text{OH}$ in each system was measured under the above optimal conditions. As shown in Figure 6A, the production rates of $\cdot\text{OH}$ on $\text{TiO}_2\text{-SnO}_2$ -graphite plate, TiO_2 -graphite plate and graphite plate were 0.08 mmol/L/h, 0.06mmol/L/h and 0.03mmol/L/h, respectively. Therefore, it can be concluded that the difference in $\cdot\text{OH}$ production rate is the direct cause of the difference in phenol degradation rate, COD removal rate and intermediate product concentration of the above three working electrodes.

In order to further verify the electrochemical degradation mechanism of phenol, $\text{TiO}_2\text{-SnO}_2$ -graphite plate was used as the anode to add 4 kinds of exogenous hydroxyl organic compounds (glucose, glycerol, tert-butanol and n-propanol) into the phenol system. Effluents discharged from the textile industries, leather tanning industries, paper productions and food industries contain high color and COD concentration, posing a negative effect on ecological environment. Dyes can be classified by chromophore group, and azo derivatives are perhaps the major compounds utilized in industries [53–55]. As shown in Figure 6B, the degradation rate of phenol was slightly improved after adding these four different hydroxyl compounds into the system compared with the blank system. For example, when electrolysis was conducted for 60 min, the degradation rate of phenol was increased by 13.3%, 20.6%, 13.2% and 11.7% with the addition of glucose, glycerol, tert-butanol and n-propanol, respectively.

Figure 6C shows the change rule of total COD with the extension of electrochemical oxidation time of phenol after adding four hydroxyl compounds. It can be seen that the removal effect of total COD is the most obvious after the addition of glycerin to the system. The change of COD after the addition of tert-butanol is relatively complex, and the COD removal rate gradually increases before 90 min, which is higher than that of glucose and n-propanol systems. The removal rate at 4h was between glucose and n-propanol. The COD removal rate of n-propanol system was the worst. After 4 h reaction, COD removal rates of glycerol, tert-butanol, glucose and n-propanol were 74.7%, 26.8%, 31.7% and 25.9%, respectively.

Figure 6D shows the change rule of the remaining COD after deducting the COD of corresponding phenol. It can be seen that COD removal rate of glycerin system is still the highest. After 4h reaction, COD removal rates were 63.4%, 3.5%, -4.5% and -49.7% respectively. Different from Figure 6C, the COD removal rate of each hydroxyl compound was lower than that of the corresponding COD in Figure 6C. The COD removal rate of n-propyl alcohol and tert-butanol was negative, which indicated that the electrochemical system had a certain selectivity for degradation of different hydroxyl organic compounds. However, the COD removal rate of tert-butanol system showed a negative growth trend with the extension of electrolysis time, which may be because tert-butanol inhibited the production of $\cdot\text{OH}$, so that the degradation of phenol produced a series of intermediate products which accumulated in the system and led to the increase of COD [56–61].

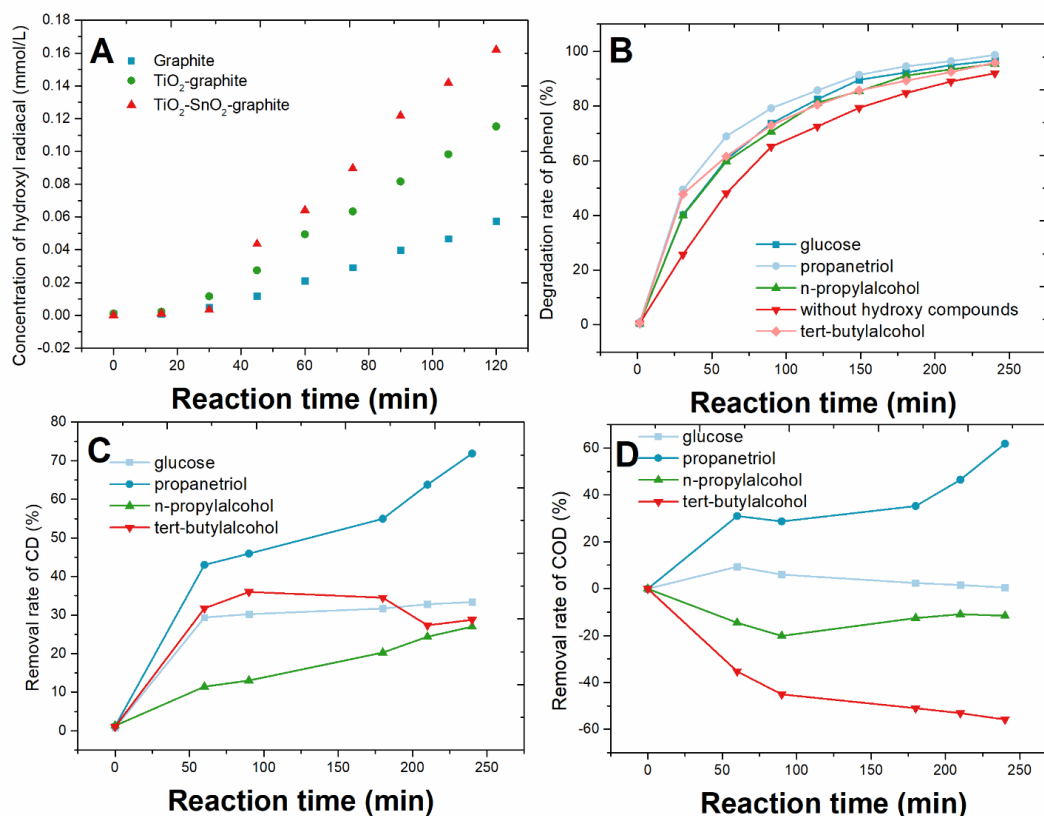


Figure 6. (A) The generation rate of hydroxyl radical on graphite plate, TiO₂-graphite plate and TiO₂-SnO₂-graphite plate. (B) Degradation rate, (C) removal rate of COD and (D) removal changes of COD when using TiO₂-SnO₂-graphite plate as anode with the presence of various of oxy-compounds.

4. CONCLUSION

In this paper, nano TiO₂-SnO₂-graphite plate was prepared by sol-gel-adsorption method, and then used as anode to establish a new electrochemical oxidation system. The degradation process conditions of TiO₂-SnO₂-graphite plate, TiO₂-graphite plate and graphite plate on phenol and the corresponding degradation rate and COD removal rate were systematically investigated. The variation of intermediate product and its concentration and ·OH production rate with electrolysis time was also discussed.

ACKNOWLEDGEMENTS

This work was financially supported by Technology Project of Tianjin Science (18YFZCSF00640).

References

1. T. Leivisk, M.K. Khalid, A. Sarpola, J. Tanskanen, *Journal of Environmental Management*, 190 (2017) 231
2. Y. Wang, S.H. Ho, C.L. Cheng, W.Q. Guo, J.S. Chang, *Bioresour. Technol.*, 222 (2016) 485.

3. A. El-Tayeb, A.H. El-Shazly, M.F. Elkady, A.B. Abdel-Rahman, *Plasma Physics Reports*, 42 (2015) 887.
4. L. Bilińska, M. Gmurek, S. Ledakowicz, *Chemical Engineering Journal*, 306 (2011) 550.
5. B. Zhang, X. Xu, L. Zhu, *Scientific Reports*, 7 17930.
6. G. Ran, Q. Li, *RSC Advances*, 9 (2019) 25414.
7. S.A. Deowan, F. Galiano, J. Hoinkis, D. Johnson, S.A. Altinkaya, B. Gabriele, N. Hilal, E. Drioli, A. Figoli, *Journal of Membrane Science* 5 (2017) S0376738816301296.
8. M. Kokko, F. Bayerk?hler, J. Erben, R. Zengerle, Ph. Kurz, S. Kerzenmacher, *Applied Energy*, 190 (2015) 1221.
9. K. Hayat, S. Menhas, J. Bundschuh, H.J. Chaudhary, *Journal of Cleaner Production*, 151 (1997) 427
10. J. Liu, K. Huang, K. Xie, Y. Yang, H. Liu, *Water Research*, 93 (2015) 187.
11. Sultan, Misbah, *Environmental Chemistry Letters*, 15 (2018) 347.
12. H. Liu, Z. Wang, H. Li, H. Wang, R. Yu, *Materials Research Bulletin*, 100 (2017) 302.
13. M. Tsuchikawa, A. Takao, T. Funaki, H. Sugihara, K. Ono, *Rsc Advances*, 7 (2017) 36612.
14. Y. Ma, J. Wang, S. Xu, Z. Zheng, J. Du, S. Feng, J. Wang, *Rsc Advances*, 7 (2017). 4014
15. J. Gao, V. Oloibiri, M. Chys, W. Audenaert, B. Decostere, Y. He, H. Van Langenhove, K. Demeestere, S.W.H. Van Hulle, *Reviews in Environmental Science & Bio/Technology*, 14 (2015) 93.
16. A. Ungurianu, Margină D, Grădinaru D, Băcanu C, Ilie M, Tsitsimpikou C, Tsarouhas K, Spandidos DA, Tsatsakis AM, *Molecular Medicine Reports*, 15 (2017) 256.
17. C.T. Sun, L.I. Yu, Q. Zhang, Z.H. Xue, *Journal of North University of China*, 36 (2015) 182.
18. I. Ghorbel, S. Maktouf, N. Fendri, K. Jamoussi, S. Ellouze Chaabouni, T. Boudawara, N. Zeghal, *Environmental Toxicology* 6 (2004) 115.
19. W. Guan, S. Tian, *Journal of Nanoelectronics & Optoelectronics* 4 (2017) 151.
20. Q. Liu, M. Zhang, T. Lv, H. Chen, A.O. Chika, C. Xiang, M. Guo, M. Wu, J. Li, L. Jia, *Bioresource Technology*, 241 (2016) 1022.
21. Y. Gründer, M.D. Fabian, S.G. Booth, D. Plana, D.J. Fermín, P.I. Hill, R.A.W. Dryfe, *Electrochimica Acta*, 110 (2019) 809.
22. R.M. Bullock, A.M. Appel, M.L. Helm, *Chemical Communications*, 50 (2019) 3125.
23. S. Trasatti, *Electrochimica Acta*, 45 (2000) 2377.
24. C.D.A. Brady, E.J. Rees, G.T. Burstein, *Journal of Power Sources*, 179 (2018) 17.
25. A. Cuesta, *Chemphyschem*, 12 (2011) 2375–2385.
26. L. Kong, X. Peng, X. Hu, J. Chen, Z. Xia, *Environmental Science & Technology*, 52 (2018) 10719.
27. E. Kerasioti, Z. Terzopoulou, O. Komini, I. Kafantaris, S. Makri, D. Stagos, K. Gerasopoulos, N.Y. Anisimov, A.M. Tsatsakis, D. Kouretas, *Toxicology Reports*, 4 (2017) 364.
28. E. Giannakopoulos, E. Isari, K. Bourikas, H. Karapanagioti, G. Psarras, G. Oron, I. Kalavrouziotis, *Journal of Environmental Management*, 195 (2017) 186.
29. N. Jaafarzadeh, F. Ghanbari, M. Alvandi, *Sustainable Environment Research*, 27 (2017) 223.
30. L. Xia, J. Bai, J. Li, L. Li, S. Chen, Q. Xu, B. Zhou, *Chemosphere*, 201 (2018) 59.
31. M. Abargues, J. Giménez, J. Ferrer, A. Bouzas, A. Seco, *Chemical Engineering Journal*, 334 (2018) 313.
32. X. Hu, Q. Zhu, Z. Gu, N. Zhang, N. Liu, M.S. Stanislaus, D. Li, Y. Yang, *Ultrasonics Sonochemistry*, 36 (2017) 301.
33. G. Moussavi, M. Pourakbar, E. Aghayani, M. Mahdavianpour, *Chemical Engineering Journal*, 350 (2018) 673.
34. B. Kakavandi, A.A. Babaei, *RSC Advances*, 6 (2016) 84999.
35. J. Rodríguez-Chueca, S.I. Moreira, M.S. Lucas, J.R. Fernandes, P.B. Tavares, A. Sampaio, J.A. Peres, *Journal of Cleaner Production*, 149 (2017) 805.
36. M. Ahmadi, F. Ghanbari, *Environmental Science and Pollution Research*, 25 (2018) 6003.

37. A.R. Abate, D. Lee, T. Do, C. Holtze, D.A. Weitz, *Lab on a Chip*, 8 (2008) 516.
38. G. Deng, C. Tang, F. Li, H. Jiang, Y. Chen, *Macromolecules*, 43 (2010) 1191.
39. B. Boury, R.J. Corriu, *Chemical Communications* (2002) 795.
40. J. Yu, X. Zhao, Q. Zhao, *Journal of Materials Science Letters*, 19 (2000) 1015.
41. W. Gang, Z. Yuanjing, X. Rongchun, *Science in China Series B: Chemistry*, 46 (2003) 184.
42. L. Wang, Y. Hu, P. Li, Y. Zhang, Q. Yan, Y. Zhao, *Chemical Engineering Journal*, 215 (2013) 157.
43. H. Wang, Q. Guan, J. Li, T. Wang, *Catalysis Today*, 236 (2014) 12.
44. E. El-Ashtoukhy, Y. El-Taweel, O. Abdelwahab, E. Nassef, *Int. J. Electrochem. Sci*, 8 (2013) 1534.
45. Q. Guan, H. Wang, J. Li, X. Li, Y. Yang, T. Wang, *Journal of Water Sustainability*, 3 (2013) 17.
46. G. Jing, L. Youzhi, C. Lingfei, *China Petroleum Processing and Petrochemical Technology*, 14 (2012) 71.
47. M. Ahmadi, H. Amiri, S.S. Martínez, *Desalination and Water Treatment*, 39 (2012) 176.
48. J.H. Naumczyk, M.A. Kucharska, *Journal of Environmental Science and Health, Part A*, 52 (2017) 649.
49. B. Wang, Y. Hu, H. Wu, S. Licht, *ECS Electrochemistry Letters*, 2 (2013) H34.
50. O. Ganzenko, D. Huguenot, E.D. Van Hullebusch, G. Esposito, M.A. Oturan, *Environmental Science and Pollution Research*, 21 (2014) 8493.
51. S. Vasudevan, M.A. Oturan, *Environmental Chemistry Letters*, 12 (2014) 97.
52. X. Wu, X. Yang, D. Wu, R. Fu, *Chemical Engineering Journal*, 138 (2008) 47.
53. A. Sáenz-Mendoza, P. Zamudio-Flores, G. Palomino-Artalejo, J. Tirado-Gallegos, V. García-Cano, J. Ornelas-Paz, C. Ríos-Velasco, C. Acosta-Muñiz, A. Vargas-Torres, R. Salgado-Delgado, *Revista Mexicana de Ingeniería Química*, 18 (2019) 39.
54. C. Hernández-Téllez, M. Cortez-Rocha, A. Burgos-Hernández, E. Rosas-Burgos, J. Lizardi-Mendoza, W. Torres-Arreola, M. Burboa-Zazueta, M. Plascencia-Jatomea, *Revista Mexicana de Ingeniería Química*, 17 (2018) 897.
55. D. Martínez-Garza, R. Reyes-Trejo, S. García-Lara, H. Mújica-Paz, A. Valdez-Fragoso, *Revista Mexicana de Ingeniería Química*, 17 (2018) 669.
56. C. López, M. Brikgi, A. García, L. García, *Revista Mexicana de Ingeniería Química*, 18 (2019) 289.
57. M. Chávez-Gutiérrez, F. Pérez-Ortega, M. Felisberti, *Revista Mexicana de Ingeniería Química*, 17 (2018) 533.
58. C. López, A. García, M. Ríos, M. Pérez, J. Román, L. García, A. Villarroel, *Revista Mexicana de Ingeniería Química*, 17 (2018) 75.
59. R. Zambrano-Rangel, V. Rico-Ramirez, G. Iglesias-Silva, *Revista Mexicana de Ingeniería Química*, 18 (2019) 621.
60. M. Ramos-García, S. Bautista-Baños, R. González-Soto, *Revista Mexicana de Ingeniería Química*, 17 (2018) 1.
61. M. Martínez-Rico, J. Aguilar-Pliego, J. Pérez-Pariente, C. Márquez, M. Viniegra, N. Martín, *Revista Mexicana de Ingeniería Química*, 17 (2018) 523.